

晶格匹配 $\text{In}_{0.17}\text{Al}_{0.83}\text{N}/\text{GaN}$ 异质结电容散射机制

任舰 苏丽娜 李文佳

Capacitance scattering mechanism in lattice-matched $\text{In}_{0.17}\text{Al}_{0.83}\text{N}/\text{GaN}$ heterojunction Schottky diodes

Ren Jian Su Li-Na Li Wen-Jia

引用信息 Citation: *Acta Physica Sinica*, 67, 247202 (2018) DOI: 10.7498/aps.67.20181050

在线阅读 View online: <http://dx.doi.org/10.7498/aps.67.20181050>

当期内容 View table of contents: <http://wulixb.iphy.ac.cn/CN/Y2018/V67/I24>

您可能感兴趣的其他文章

Articles you may be interested in

[Ni/Au/n-GaN 肖特基二极管可导位错的电学模型](#)

Physical model of conductive dislocations in GaN Schottky diodes

物理学报.2018, 67(17): 177202 <http://dx.doi.org/10.7498/aps.67.20180762>

[氮化镓基感光栅极高电子迁移率晶体管器件设计与制备](#)

Design and fabrication of high electron mobility transistor devices with gallium nitride-based

物理学报.2017, 66(24): 247203 <http://dx.doi.org/10.7498/aps.66.247203>

[加载功率与壳温对 AlGaIn/GaN 高速电子迁移率晶体管器件热阻的影响](#)

Influence of power dissipation and case temperature on thermal resistance of AlGaIn/GaN high-speed electron mobility transistor

物理学报.2016, 65(7): 077201 <http://dx.doi.org/10.7498/aps.65.077201>

[金属有机物化学气相沉积生长 GaN 薄膜的室温热电特性研究](#)

Room-temperature thermoelectric properties of GaN thin films grown by metal organic chemical vapor deposition

物理学报.2015, 64(4): 047202 <http://dx.doi.org/10.7498/aps.64.047202>

[新型 AlGaInP 系发光二极管饱和特性与寿命的研究](#)

Investigation of the saturation characteristic and lifetime of the novel AlGaInP lightemitting diodes

物理学报.2014, 63(3): 037201 <http://dx.doi.org/10.7498/aps.63.037201>

晶格匹配 $\text{In}_{0.17}\text{Al}_{0.83}\text{N}/\text{GaN}$ 异质结 电容散射机制*

任舰[†] 苏丽娜 李文佳

(淮阴师范学院物联网工程系, 淮安 223600)

(2018年5月29日收到; 2018年11月1日收到修改稿)

制备了晶格匹配 $\text{In}_{0.17}\text{Al}_{0.83}\text{N}/\text{GaN}$ 异质结圆形平面结构肖特基二极管, 通过测试和拟合器件的电容-频率曲线, 研究了电容的频率散射机制. 结果表明: 在频率高于200 kHz后, 积累区电容随频率出现增加现象, 而传统的电容模型无法解释该现象. 通过考虑漏电流、界面态和串联电阻等影响对传统模型进行修正, 修正后的电容频率散射模型与实验结果很好地符合, 表明晶格匹配 $\text{In}_{0.17}\text{Al}_{0.83}\text{N}/\text{GaN}$ 异质结电容随频率散射是漏电流、界面态和串联电阻共同作用的结果.

关键词: 晶格匹配, $\text{In}_{0.17}\text{Al}_{0.83}\text{N}/\text{GaN}$ 异质结, 电容频率散射

PACS: 72.80.Ey, 73.40.Kp, 73.40.-c

DOI: 10.7498/aps.67.20181050

1 引言

与传统窄禁带半导体相比, 以GaN为代表的宽禁带III族氮化物具有高电子饱和速度、高击穿电场与高热稳定性等优越的物理特性. 因此, GaN材料及其异质结构非常适合用来制备高频大功率电子器件^[1-3]. 特别是自发极化效应显著的晶格匹配 $\text{In}_{0.17}\text{Al}_{0.83}\text{N}/\text{GaN}$ 异质结, 由于能在界面处诱导高浓度的二维电子气(2DEG), 逐渐成为高电子迁移率晶体管(HEMT)的核心结构^[4-6]. 但是, 晶格匹配 $\text{In}_{0.17}\text{Al}_{0.83}\text{N}/\text{GaN}$ HEMT的广泛应用仍然受到电流崩塌效应的限制, 在高频模式下工作时, 器件输出功率无法达到理论预测值^[7-9]. 在传统硅基金属氧化物半导体(MOS)器件中, 电流崩塌主要由材料中的缺陷态引起, 研究人员通过电容-电压($C-V$)曲线的频率散射行为来表征缺陷态的密度^[10-12]. 但是, 由于材料特性之间的差异, 晶格匹配 $\text{In}_{0.17}\text{Al}_{0.83}\text{N}/\text{GaN}$ HEMT的电容频率散射机制与硅基MOS器件并不相同, 为了准确地表征缺陷态, 抑制电流崩塌, 需要正确地解释其电容频率散射机制.

鉴于此, 本文首先制备了方便测试电容的圆形平面结构的晶格匹配 $\text{In}_{0.17}\text{Al}_{0.83}\text{N}/\text{GaN}$ 异质结肖特基二极管, 该结构与HEMT具有等效的栅极电流电容特性; 然后通过测试和拟合器件变频电容-频率($C-f$)特性, 分析了晶格匹配 $\text{In}_{0.17}\text{Al}_{0.83}\text{N}/\text{GaN}$ 异质结的电容频率散射机制.

2 器件制备与测试

采用金属有机化合物气相沉积法在蓝宝石衬底上制备晶格匹配 $\text{In}_{0.17}\text{Al}_{0.83}\text{N}/\text{GaN}$ 异质结肖特基二极管, 其外延结构如图1(a)所示, 主要包括3 μm 非掺杂GaN层、18 nm非掺杂 $\text{In}_{0.17}\text{Al}_{0.83}\text{N}$ 势垒层和1 nm AlN隔离层. GaN层生长温度为940 $^{\circ}\text{C}$, 压力为40 Torr (1 Torr \approx 133.322 Pa), NH_3 流量为1500 sccm (1 sccm = 1 mL/min), V/III比为3250. InAlN层生长温度为760 $^{\circ}\text{C}$, 压力为200 Torr, TMAI, TMIIn和 NH_3 流量分别为2.3 $\mu\text{mol}/\text{min}$, 5.8 $\mu\text{mol}/\text{min}$ 和1200 sccm, V/III比为6610. 在图1(b)所示的器件平面照片中, 圆形肖特基电极采用Pt/Au, 直径为100 μm , 与欧

* 江苏省高校自然科学基金项目(批准号: 17KJB510007, 17KJB535001)资助的课题.

[†] 通信作者. E-mail: 916181396@qq.com

姆电极的间距为 20 μm , 其微图形采用标准光刻与剥离 (lift-off) 技术定义; Ti/Al/Ti/Au 欧姆接触采用在 870 $^{\circ}\text{C}$ 的 N_2 氛围中退火 30 s 获得, 且表面覆盖了 150 nm SiN 介质; 测试电极电镀 2 μm 金进行加厚, 隔离采用台面隔离. 利用 Keithley 4200 SCS 精密半导体参数分析仪测量晶格匹配 $\text{In}_{0.17}\text{Al}_{0.83}\text{N}/\text{GaN}$ 异质结肖特基二极管的电流-电压 (I - V) 和 C - V 特性, 根据室温 C - V (1 MHz) 曲线计算, 获得 InAlN/GaN 异质界面的 2DEG 面密度约为 $1.23 \times 10^{13} \text{ cm}^{-2}$ [13].

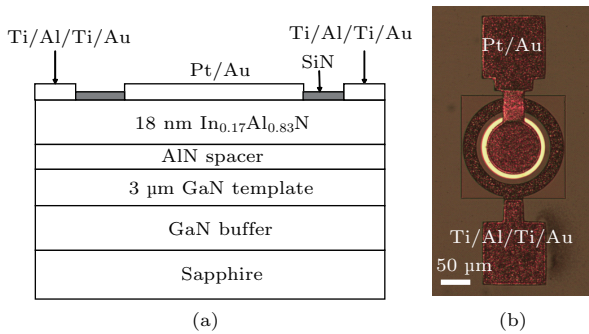


图 1 InAlN/GaN 异质结肖特基二极管的 (a) 横截面示意图和 (b) 光学显微照片
Fig. 1. (a) Schematic cross-section and (b) optical micrograph of the fabricated InAlN/GaN heterojunction Schottky diode.

3 结果与讨论

图 2 所示分别为低频和高频下的晶格匹配 $\text{In}_{0.17}\text{Al}_{0.83}\text{N}/\text{GaN}$ 肖特基二极管 C - V 频率散射特性. 由图 2(a) 可以看出, 随着频率由 50 kHz 逐渐增加到 250 kHz, 器件积累区电容随频率的增加而逐渐降低, 该现象符合传统的 HEMT 器件电容频率散射特性 [14-16]. 然而, 随着频率继续增加, 积累区电容随频率的增加而快速增加, 出现电容强散射现象 (如图 2(b) 所示). 通常情况下, 电容频率散射行为主要由界面态和势垒层缺陷态导致. 但是, 根据传统观点, 器件电容随着频率增加应单调减少. 很显然, 缺陷态行为无法解释高频下电容随频率强散射现象. 由于晶格匹配 $\text{In}_{0.17}\text{Al}_{0.83}\text{N}/\text{GaN}$ 异质结器件是一种重要的高频大功率应用器件, 高频散射将直接影响其高频工作的可靠性, 所以很有必要对该现象进行研究.

图 3 所示为零偏压下晶格匹配 $\text{In}_{0.17}\text{Al}_{0.83}\text{N}/\text{GaN}$ 异质结肖特基二极管的 C - f 曲线 (频率变化范围为 10 kHz 至 1 MHz). 可以看出, 随着频率逐渐

增加, 电容先缓慢减小, 随后快速增加, 高频散射非常明显. 该现象会导致器件截止频率和最大振荡频率的降低, 影响其高频工作的稳定性. 下面将通过数据拟合的方法, 分析产生该现象的原因.

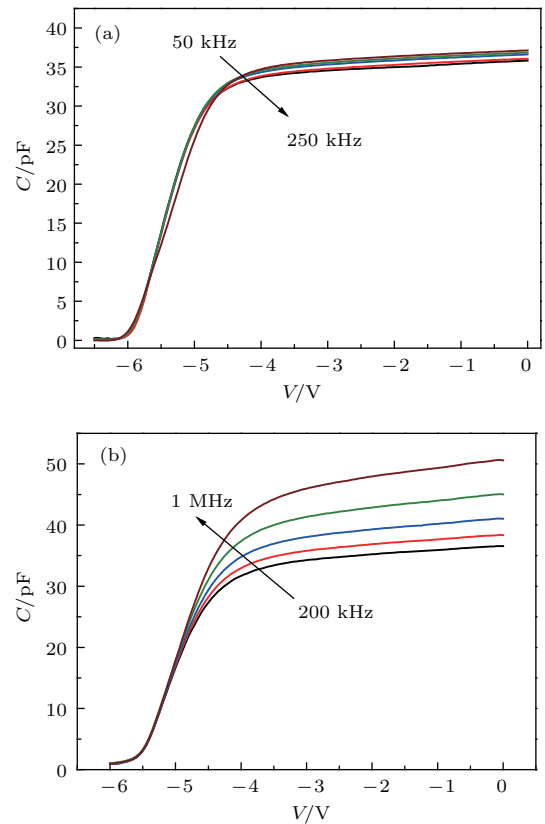


图 2 晶格匹配 $\text{In}_{0.17}\text{Al}_{0.83}\text{N}/\text{GaN}$ 肖特基二极管的 C - V 频率散射特性 (a) 低频; (b) 高频
Fig. 2. C - V frequency scattering characteristics of lattice-matched $\text{In}_{0.17}\text{Al}_{0.83}\text{N}/\text{GaN}$ heterojunction Schottky diode: (a) Low frequency; (b) high frequency.

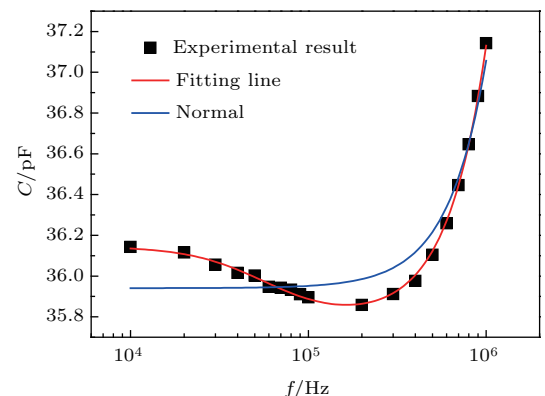


图 3 晶格匹配 $\text{In}_{0.17}\text{Al}_{0.83}\text{N}/\text{GaN}$ 肖特基二极管电容的频率依赖特性
Fig. 3. Frequency dependence of the capacitance in lattice-matched $\text{In}_{0.17}\text{Al}_{0.83}\text{N}/\text{GaN}$ heterostructure Schottky diode.

图 4(a) 所示为测试模型, 其等效阻抗 Z 可表示为

$$Z = \frac{R_m}{1 + (R_m \omega C_m)^2} - j \frac{R_m^2 \omega C_m}{1 + (R_m \omega C_m)^2}, \quad (1)$$

其中, R_m 和 C_m 分别为测试模型等效电路的电阻、电容; ω 为角频率.

Miller 等^[17]指出, GaN 材料中存在较高的界面态缺陷密度, 界面态和串联电阻共同作用会导致 AlGaIn/GaN HEMT 产生电容频率散射行为. 其模

$$C_m = \left\{ \frac{\left[R_S + \frac{R_P}{1 + (R_P \omega C_P)^2} \right]^2}{\left[\frac{1}{\omega^2 C_B} + \frac{R_P^2 C_P}{1 + (R_P \omega C_P)^2} \right]} + \frac{1}{\omega C_B} + \frac{R_P^2 \omega C_P}{1 + (R_P \omega C_P)^2} \right\}^{-1}. \quad (3)$$

考虑到晶格匹配 In_{0.17}Al_{0.83}N/GaN HEMT 的器件结构与 AlGaIn/GaN HEMT 相似, 因此该模型被用来拟合 C - f 实验数据. 拟合发现, 该模型中电容随频率增加单调减小, 显然该模型对解释晶格匹配 In_{0.17}Al_{0.83}N/GaN HEMT 积累区电容增加现象不适用.

Yang 和 Hu^[18]指出, 在硅基 MOS 中电容频率散射现象主要受到漏电流和串联电阻影响, 其模型等效电路如图 4(c) 所示. 其中 R_B 为流过势垒电流的等效电阻. 根据上述模型, 电容测量阻抗 Z 可表示为

$$Z = R_S + \frac{R_B}{1 + (R_B \omega C_B)^2} - j \frac{R_B^2 \omega C_B}{1 + (R_B \omega C_B)^2}, \quad (4)$$

观测电容 C_m 可表示为

$$C_m = \left\{ \frac{\left[R_S + \frac{R_B}{1 + (R_B \omega C_B)^2} \right]^2}{\left[\frac{R_B^2 C}{1 + (R_B \omega C_B)^2} \right]} + \frac{R_B^2 \omega C}{1 + (R_B \omega C_B)^2} \right\}^{-1}. \quad (5)$$

使用该模型对实验 C - f 曲线进行拟合, 发现该模型无法拟合实验数据, 结果如图 3 中蓝色实线所示, 该模型无法拟合实验数据, 因此该模型也不适用.

图 5 所示为室温 (300 K) 下测得的 C - V 曲线, 内插图为相同器件的 I - V 曲线. 由图 5 可观察到以下特性: 随着反向偏压从 0 V 逐渐增加到 6 V, 由于异质界面的高浓度 2DEG 逐渐被耗尽, 电容随偏压逐渐降低. 同样地, 内插图中器件反向漏

型的等效电路如图 4(b) 所示, 其中 C_B 为势垒电容, R_S 为串联电阻, C_P 和 R_P 分别为界面缺陷态等效电阻和等效电容. 根据该模型, 电容测量阻抗 Z 可表示为

$$Z = R_S - j \frac{1}{\omega C_B} + \frac{R_P}{1 + (R_P \omega C_P)^2} - j \frac{R_P^2 \omega C_P}{1 + (R_P \omega C_P)^2}. \quad (2)$$

观测电容 C_m 可表示为

电流也在 6 V 时达到饱和. 可以看出, 晶格匹配 In_{0.17}Al_{0.83}N/GaN 异质结反向具有高达 10^{-4} A 的

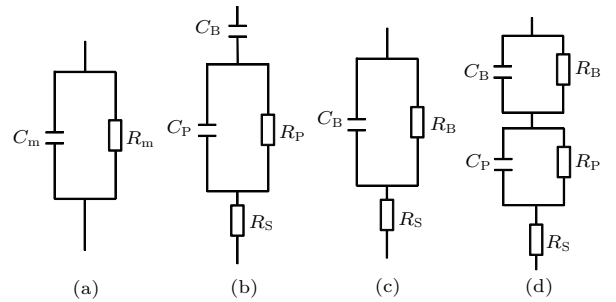


图 4 电容散射等效模型

Fig. 4. Equivalent models of capacitance scattering mechanism.

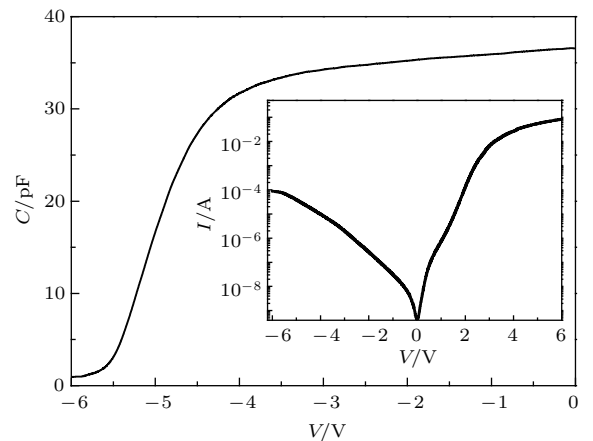


图 5 InAlN/GaN 异质结肖特基二极管的室温 C - V 特性 (1 MHz), 其中内插图为 I - V 特性

Fig. 5. C - V characteristic of InAlN/GaN heterojunction Schottky diode measured at room temperature (1 MHz) with the I - V characteristics plotted in the inset.

漏电流, 并且晶格匹配 $\text{In}_{0.17}\text{Al}_{0.83}\text{N}/\text{GaN}$ 异质结的电容与反向漏电流之间存在直接联系. 由于 InAlN 材料中存在强极化效应, 由此产生的极化电场通常高达 10^7 V/cm, 强极化电场会压缩能带形成近三角势垒, 从而发生 Fowler-Nordheim 隧穿, 并形成大漏电流^[19]. 由此我们认为在 InAlN/GaN 异质结中, 较大的漏电流是不可忽视的因素. 综合上面两个模型, 本文对强积累区电容散射模型进行修

正, 该模型等效电路如图 4(d) 所示. 根据该模型, 电容测量阻抗 Z 可表示为

$$Z = R_s + \frac{R_B}{1 + (R_B\omega C_B)^2} - j \frac{R_B^2\omega C_B}{1 + (R_B\omega C_B)^2} + \frac{R_P}{1 + (R_P\omega C_P)^2} - j \frac{R_P^2\omega C_P}{1 + (R_P\omega C_P)^2}, \quad (6)$$

观测电容 C_m 可表示为

$$C_m = \left\{ \frac{\left[R_s + \frac{R_B}{1 + (R_B\omega C_B)^2} + \frac{R_P}{1 + (R_P\omega C_P)^2} \right]^2}{\left[\frac{R_B^2 C_B}{1 + (R_B\omega C_B)^2} + \frac{R_P^2 C_P}{1 + (R_P\omega C_P)^2} \right]} + \frac{R_B^2\omega C_B}{1 + (R_B\omega C_B)^2} + \frac{R_P^2\omega C_P}{1 + (R_P\omega C_P)^2} \right\}^{-1}. \quad (7)$$

使用该模型对实验 C - f 曲线进行拟合, 拟合结果如图 3 中红色实线所示. 可以看出, 修正后的模型拟合结果与实验结果符合得很好. 其中, 几个重要的参数拟合结果分别为: $R_s = 50 \Omega$, $R_B = 817.5 \Omega$, $C_B = 4.04 \times 10^{-11}$ F, 参数量级基本符合文献报道值^[20]. 拟合得到 C_P 和 R_P 结果分别为: $C_P = 2.65 \times 10^{-5}$ F, $R_P = 0.1 \Omega$, 根据界面等效电容与界面缺陷密度关系 $C_P = qD_P$, 得到界面缺陷密度约为 $1.66 \times 10^{10} \text{ cm}^{-2} \cdot \text{eV}^{-1}$, 根据时间常数计算方法 $\tau_P = R_P C_P$, 得到时间常数为 $2.65 \mu\text{s}$. 根据 Semra 等^[21] 的报道, AlGaIn/GaN 异质界面缺陷密度量级约为 10^{11} — $10^{12} \text{ cm}^{-2} \cdot \text{eV}^{-1}$, 时间常数为 $1 \mu\text{s}$ — 3 ms , 本文获得的缺陷密度值略低于 AlGaIn/GaN 异质结报道结果, 但考虑到 InAlN 与 GaN 异质界面实现了晶格匹配, 理论上 InAlN/GaN 异质界面缺陷密度低于 AlGaIn/GaN , 因此拟合获得的结果具有一定的合理性. 为了获得界面等效电容和等效电阻值, 拟合时不得不假定界面等效电容 C_P 和等效电阻 R_P 不随频率变化. 因此, 我们认为晶格匹配 $\text{In}_{0.17}\text{Al}_{0.83}\text{N}/\text{GaN}$ HEMT 积累区观察到的电容散射是漏电流、界面态和串联电阻共同影响的结果.

4 结 论

本文研究了晶格匹配 $\text{In}_{0.17}\text{Al}_{0.83}\text{N}/\text{GaN}$ 异质结肖特基二极管的强积累区电容频率散射机制. 考虑多种因素后对器件变频 C - f 特性进行拟合, 通过分析发现电容的频率散射是漏电流与界面态俘获电子共同作用的结果. 该研究结果将进一步推动

InAlN/GaN 异质结器件在高频大功率领域的应用.

参考文献

- [1] Wang C, Zhao M D, Pei J Q, He Y L, Li X D, Zheng X F, Mao W, Ma X H, Zhang J C, Hao Y 2016 *Acta Phys. Sin.* **65** 038501 (in Chinese) [王冲, 赵梦荻, 裴九清, 何云龙, 李祥东, 郑雪峰, 毛维, 马晓华, 张进成, 郝跃 2016 物理学报 **65** 038501]
- [2] Li S P, Zhang Z L, Fu K, Yu G H, Cai Y, Zhang B S 2017 *Acta Phys. Sin.* **66** 197301 (in Chinese) [李淑萍, 张志利, 付凯, 于国浩, 蔡勇, 张宝顺 2017 物理学报 **66** 197301]
- [3] Sun M, Zhang Y, Gao X, Tomas P 2017 *IEEE Electron Dev. Lett.* **38** 509
- [4] Xue J S, Hao Y, Zhang J C, Zhou X W, Liu Z Y 2011 *Appl. Phys. Lett.* **98** 113504
- [5] Li Q, Chen Q, Zhong J 2018 *Acta Phys. Sin.* **67** 027303 (in Chinese) [李群, 陈谦, 钟景 2018 物理学报 **67** 027303]
- [6] Xing W, Liu Z, Ranjan K, Tomas P 2018 *IEEE Electron Dev. Lett.* **39** 947
- [7] Kuzmik J, Pozzovivo G, Abermann S, Carlin J F, Gonschorek M, Feltin E 2008 *IEEE Trans. Electron Dev.* **55** 937
- [8] Chung J W, Saadat O I, Tirado J M, Gao X 2009 *IEEE Electron Dev. Lett.* **30** 904
- [9] Li W, Wang Q, Zhan X 2016 *Semicond. Sci. Technol.* **31** 125003
- [10] Yuan Y, Wang L, Yu B, Shin B, Ahn J, McIntyre P C 2011 *IEEE Electron Dev. Lett.* **32** 485
- [11] Lin H C, Yang T, Sharifi H, Kin S K, Xuan Y 2007 *Appl. Phys. Lett.* **91** 212101
- [12] Stemmer S, Chobpattana V, Rajan S 2012 *Appl. Phys. Lett.* **100** 233510
- [13] Zhao J Z, Lin Z J, Corrigan T D, Wang Z, You Z D, Wang Z G 2007 *Appl. Phys. Lett.* **91** 173507
- [14] Stoklas R, Gregušová D, Novák J, Vescan A, Kordoš P 2008 *Appl. Phys. Lett.* **93** 124103

- [15] Xie S, Yin J, Zhang S, Liu B, Zhou W, Feng Z 2009 *Solid-State Electron.* **53** 1183
- [16] Shealy J R, Brown R J 2008 *Appl. Phys. Lett.* **92** 032101
- [17] Miller E J, Dang X Z, Wieder H H, Asbeck P M, Yu E T, Sullivan G J 2000 *J. Appl. Phys.* **87** 8070
- [18] Yang K J, Hu C 1999 *IEEE Trans. Electron Dev.* **46** 1500
- [19] Turuvekere S, Karumuri N, Rahman A A 2013 *IEEE Trans. Electron Dev.* **60** 3157
- [20] Nsele S D, Escotte L, Tartarin J, Piotrowicz S, Delage S L 2013 *IEEE Trans. Electron Dev.* **60** 1372
- [21] Semra L, Telia A, Soltani A 2010 *Surf. Interface Anal.* **42** 799

Capacitance scattering mechanism in lattice-matched $\text{In}_{0.17}\text{Al}_{0.83}\text{N}/\text{GaN}$ heterojunction Schottky diodes*

Ren Jian[†] Su Li-Na Li Wen-Jia

(Department of Internet of Things, Huaiyin normal University, Huaian 223600, China)

(Received 29 May 2018; revised manuscript received 1 November 2018)

Abstract

In order to study the frequency scattering mechanism of capacitance in latticematched $\text{In}_{0.17}\text{Al}_{0.83}\text{N}/\text{GaN}$ high electron mobility transistors (HEMTs), the latticematched $\text{In}_{0.17}\text{Al}_{0.83}\text{N}/\text{GaN}$ heterojunction Schottky diodes with circular planar structure, which have equivalent capacitance characteristics to those of HEMTs, are fabricated and tested in this paper. The experimental curves of capacitance-voltage characteristics at different frequencies show that the capacitance of the accumulation area decreases gradually with the increase of frequency at low frequency, which accords with the capacitance frequency scattering characteristics of traditional HEMT devices. However, when the frequency is higher than 200 kHz, the capacitance of the accumulation area increases rapidly with frequency increasing, which cannot be explained by the traditional capacitance model. By comparing the reverse current and capacitance characteristics of latticematched $\text{In}_{0.17}\text{Al}_{0.83}\text{N}/\text{GaN}$ Schottky diodes, it is observed that the saturation behavior of the reverse leakage current is clearly associated with full depletion of the two-dimensional electron gas at the InAlN/GaN interface, which is indicated by the rapid drop of the diode capacitance. This observation suggests that the large reverse leakage current of the lattice-matched $\text{In}_{0.17}\text{Al}_{0.83}\text{N}/\text{GaN}$ Schottky diode, which reaches up to 10^{-4} A, should have a direct influence on the capacitance scattering. By considering the influence of leakage current, interface state and series resistance comprehensively, the capacitance frequency scattering model is modified based on the traditional model. Using various models to fit the experimental capacitance-frequency data, the results from the modified model agree well with the experimental results. According to the parameters obtained by fitting, the density and the time constant of interface defects in latticematched $\text{In}_{0.17}\text{Al}_{0.83}\text{N}/\text{GaN}$ Schottky diodes, determined by equivalent interface capacitance and resistance, are about $1.66 \times 10^{10} \text{ cm}^{-2} \cdot \text{eV}^{-1}$ and $2.65 \mu\text{s}$, respectively. According to the values reported in the literature, it is suggested that the modified capacitance frequency scattering model should be reasonable for explaining the capacitance scattering phenomenon in accumulation area. In conclusion, we believe that the capacitance of latticematched $\text{In}_{0.17}\text{Al}_{0.83}\text{N}/\text{GaN}$ Schottky diode scatters is a joint result of leakage current, interface state and series resistance. The interface defects in $\text{In}_{0.17}\text{Al}_{0.83}\text{N}/\text{GaN}$ Schottky diodes usually have a great influence on frequency and power characteristics of devices, a correct explanation for the frequency scattering mechanism of capacitance is the basis for determining the locations and sources of defects in III nitride devices.

Keywords: lattice-matched, $\text{In}_{0.17}\text{Al}_{0.83}\text{N}/\text{GaN}$ heterojunction, frequency scattering mechanism of capacitance

PACS: 72.80.Ey, 73.40.Kp, 73.40.-c

DOI: 10.7498/aps.67.20181050

* Project supported by the Natural Science Foundation of the Jiangsu Higher Education Institutions of China (Grant Nos. 17KJB510007, 17KJB535001).

[†] Corresponding author. E-mail: 916181396@qq.com